

## Boundary element analysis of the frictionless indentation of piezoelectric films

Luis Rodríguez-Tembleque , Federico C. Buroni  and Andrés Sáez 

Escuela Técnica Superior de Ingeniería, Universidad de Sevilla, Camino de los Descubrimientos s/n, Sevilla E-41092, Spain

### ABSTRACT

The boundary element method is used for studying frictionless indentation response of piezoelectric (PE) films under spherical indenter (i.e. sphere) and circular cylindrical indenter (i.e. punch). An augmented Lagrangian formulation is employed to solve PE films of finite thickness under contact conditions. The methodology is validated by comparison with theoretical solutions presented in the literature for the two limiting cases: infinitely thick and infinitely thin PE films closed-form solutions. Furthermore, the formulation is applied to compute the indentation response of those cases in between.

### ARTICLE HISTORY

Received 23 October 2015  
Accepted 27 February 2016

### KEYWORDS

Piezoelectric;  
indentation; conducting  
electrical boundary  
condition; contact  
mechanics; boundary  
element method

## Introduction

Piezoelectric (PE) materials are widely used in the development of high technological applications such as actuators and sensors for engineering control equipment or smart structures, because of the coupling effects between mechanical and electric fields. General mathematical models for these electro-elastic materials and systems can be found in the following monographs: Cady (1946), Ikeda (1996), Ding and Chen (2001) and Yang and Yang (2005).

One of the most common shapes for sensor or actuators applications is the film form, as it can be observed from Mason (1950), Pohanka and Smith (1988), Uchino (1997) and Muralt (2008). The film is bonded to a substrate and its thickness is ranging from a few nanometres to several millimetres. To have a better understanding of the indentation behaviour of these systems and to measure the mechanical and electric properties of these materials, many researchers have been analysing these systems under different contact conditions.

Indentation techniques on bulk and film forms have been studied experimentally by: Saigal, Giannakopoulos, Pettermann and Suresh (1999), Ramamurty, Sridhar, Giannakopoulos and Suresh (1999) and Kamble, Kubair and Ramamurty (2009).

Theoretical investigations on bulk forms have been carried out by Matysiak (1985), Fan, Sze and Yang (1996), Chen and Ding (1996), Chen, Shioya and Ding

(1999), Giannakopoulos and Suresh (1999), Ding, Hou and Guo (2000), Wang, Fang and Chen (2002), Ramirez and Heyliger (2003), Ramirez (2006), Kalinin, Karapetian and Kachanov (2004), Gao and Noda (2004), Wang and Han (2006), Ke, Yang, Kitipornchai and Wang (2008) and Yang (2008).

More recently, theoretical investigations on film forms have been carried out by Wang, Chen and Lu (2008, 2011, 2012), who considered PE films under frictionless normal indentation conditions. Wang et al. (2008) studied the axisymmetric indentation problem of a PE film perfectly bonded to a rigid substrate and later Wang et al. (2011, 2012) studied the elastic substrate effect.

Numerical schemes based on the finite element method (FEM) have been also proposed to simulate electro-elastic contact under frictionless conditions by Han, Sofonea and Kazmi (2007), Barboteu, Fernández and Ouafik (2008) or Hüeber, Matei and Wohlmuth (2013). Liu and Fuqian (2012b) applied the FEM to study spherical indentation response of PE half-spaces and later Liu and Fuqian (2012a) applied the FEM to the study of the effect of electric boundary conditions on the spherical indentation of transversely isotropic PE films. The advantage of numerical methods is that the indentation studies are not restricted to axisymmetric cases or specific geometries. General geometries, material orientation or even friction can be considered and incorporated into the model (see Liu and Yang, 2013).

In this context, this work proposes the boundary element method (BEM) as an alternative to the FEM to tackle these problems. The BEM has revealed to be a very suitable and accurate numerical methodology to study contact indentation problems of anisotropic materials see (Blazquez et al. 2006 for 2D and Rodríguez-Tembleque et al. 2011 for 3D). In general, the BEM considers only the boundary degrees of freedom. So, for electro-elastic materials, as the number of degrees of freedom per node is increased due to fact that the electric field is taken into account, we obtain a significant reduction in the number of degrees of freedom when compared with the finite element formulations (specially in 3D problems).

This paper applies the boundary element formulation previously developed by Rodríguez-Tembleque et al. (2015) to study frictionless indentation response of PE bodies in the presence of electric fields (i.e. PE films bonded to a rigid substrate). The contact methodology presented in this work is based on an augmented Lagrangian formulation similar to that of Alart and Curnier (1991) and Christensen, Klarbring, Pang and Strömberg (1998), and it can be found in the monographs by Kikuchi and Oden (1988), Laursen (2002) or Wriggers (2002). The boundary elements technique is used to compute the electro-elastic influence coefficients, whilst the projection contact operators acting over the augmented Lagrangian guarantee the PE contact restrictions fulfilment. The present methodology is validated by comparison with theoretical solutions presented for infinitely thick and infinitely thin PE films by Wang et al. (2008), and then applied to compute the indentation response of those cases in between.

## Piezoelectricity

Let  $\Omega \subset \mathbb{R}^3$  be a 3D region occupied by a PE material with a piecewise smooth boundary  $\partial\Omega$ , and  $(x_i)$  ( $i = 1, 2, 3$ ) a Cartesian coordinate system. This work considers small deformations, so the infinitesimal strain tensor  $\gamma$  and the electric field  $E$  are obtained from derivatives of the displacements  $u$  and potential field  $\varphi$  as

$$\begin{aligned} \gamma_{ij} &= (u_{i,j} + u_{j,i})/2 & \text{in } \Omega, \\ E_i &= -\varphi_{,i} & \text{in } \Omega. \end{aligned} \quad (1)$$

In the absence of body forces, the mechanical stresses  $\sigma$  and the electric displacements  $D$  are divergence-free, that is,

$$\begin{aligned} \sigma_{ij,j} &= 0 & \text{in } \Omega, \\ D_{i,i} &= 0 & \text{in } \Omega, \end{aligned} \quad (2)$$

where repeated dummy indices indicate summation. In linear PE materials, the elastic and electric fields are coupled through the constitutive law

$$\begin{aligned} \sigma_{ij} &= c_{ijkl}\gamma_{kl} - e_{lij}E_l & \text{in } \Omega, \\ D_i &= e_{ikl}\gamma_{kl} + \epsilon_{il}E_l & \text{in } \Omega, \end{aligned} \quad (3)$$

where  $c$  and  $\epsilon$  denote the elastic stiffness tensor and the dielectric permittivity tensor, respectively, which are positive definite, whilst tensor  $e$  governs the PE coupling. These tensors satisfy the following symmetries:  $c_{ijkl} = c_{jikl} = c_{ijlk} = c_{klij}$ ,  $e_{kij} = e_{kji}$ ,  $\epsilon_{kl} = \epsilon_{lk}$ .

## Boundary conditions of the problem

Two partitions of the boundary  $\partial\Omega$  are considered to define the mechanical and the electrical boundary conditions. The first one divides  $\partial\Omega$  into three disjoint parts:  $\partial\Omega = \partial\Omega_u \cup \partial\Omega_t \cup \partial\Omega_c$ , being  $\partial\Omega_u \cap \partial\Omega_t \cap \partial\Omega_c = \emptyset$ . Here,  $\partial\Omega_u$  denotes the boundary on which displacements  $\tilde{u}_i$  are prescribed,  $\partial\Omega_t$  denotes the part of the boundary where tractions  $\tilde{t}_i = \sigma_{ij}v_j$  are imposed and  $\partial\Omega_c$  represents the potential contact surface under rigid indentation, which have outward unit normal vector  $v_{ci}$ . The second partition is:  $\partial\Omega = \partial\Omega_\varphi \cup \partial\Omega_q \cup \partial\Omega_c$ , where the electric potential  $\tilde{\varphi}$  is prescribed on  $\partial\Omega_\varphi$  and the electric charge  $\tilde{q} = D_i v_i$  is assumed on  $\partial\Omega_q$ .

## Boundary conditions

Mechanical and electrical boundary conditions are prescribed on  $\partial\Omega$ . The Dirichlet boundary conditions are

$$\begin{aligned} u_i &= \tilde{u}_i & \text{on } \partial\Omega_u, \\ \varphi &= \tilde{\varphi} & \text{on } \partial\Omega_\varphi, \end{aligned} \quad (4)$$

and the Neumann boundary conditions are given by

$$\begin{aligned}\sigma_{ij}v_j &= \tilde{t}_i & \text{on } \partial\Omega_t, \\ D_i v_i &= \tilde{q} & \text{on } \partial\Omega_q,\end{aligned}\quad (5)$$

with  $v_i$  being the outward unit normal to the boundary.

For a well-posed problem, either displacement or traction and electric potential or normal charge flux must be prescribed at each boundary point outside the contact zone  $\partial\Omega_c$ .

Under small displacement assumption, a common unit normal vector  $v_{ci}$  can be considered in  $\partial\Omega_c$ . So the nonlinear boundary conditions are:

$$\begin{aligned}\sigma_{ij}v_{cj} &= p_i & \text{on } \partial\Omega_c, \\ D_i v_{ci} &= -\kappa(\varphi - \varphi_o) & \text{on } \partial\Omega_c,\end{aligned}\quad (6)$$

where  $p_i$  is the contact traction,  $p_v = \mathbf{p} \cdot \mathbf{v}_c$  is the normal contact pressure,  $\kappa$  is the conductivity coefficient and  $\varphi_o$  denotes the electric potential of the foundation or the indenter. Frictionless contact is assumed, i.e.  $\mathbf{p}_\tau = \mathbf{p} - p_v \mathbf{v}_c = \mathbf{0}$ .

### Contact restrictions

The unilateral contact law involves Signorini's contact conditions in  $\partial\Omega_c$ :

$$g_v \geq 0, \quad p_v \leq 0, \quad g_v p_v = 0, \quad (7)$$

where  $g_v = (g_o - u_v)$ ,  $g_o$  being the initial gap between the bodies and  $u_v = \mathbf{u} \cdot \mathbf{v}_c$  ( $\mathbf{u}$  is the relative displacement on  $\partial\Omega_c$ ).

The normal contact constraints presented in (7) can be formulated as:

$$p_v - \mathbb{P}_{\mathbb{R}_-}(p_v^*) = 0, \quad (8)$$

where  $\mathbb{P}_{\mathbb{R}_-}(\bullet)$  is the normal projection function ( $\mathbb{P}_{\mathbb{R}_-}(\bullet) = \text{MIN}(0, \bullet)$ ) and  $p_v^* = p_v + r_v g_v$  is the augmented normal traction. The parameter  $r_v$  is the normal dimensional penalisation parameter ( $r_v \in \mathbb{R}^+$ ).

The electrical conductivity coefficient in (6) can be defined as  $\kappa = \kappa(p_v)$  what allows to describe perfect electrical contact conditions similarly to the Signorini's contact conditions,

$$\kappa(p_v) = \begin{cases} 0 & \text{if } p_v = 0, \\ \kappa^* & \text{if } p_v < 0, \end{cases} \quad (9)$$

$\kappa^*$  being the conductivity parameter similar to [Hüeber et al. \(2013\)](#) and [Rodríguez-Tembleque et al. \(2015\)](#). So, when there is no contact (i.e.  $p_v = 0$ ) on  $\partial\Omega_c$ , the normal component of the electric displacement field vanishes, and when there is contact, electrical charges appear in the electrical contact condition (6).

## Explicit boundary element formulation

In this section, the classical BEM formulation for elasticity (Brebbia and Dominguez, 1992 and Aliabadi, 2002, among others) is extended to the coupled PE problem following the work by Rodríguez-Tembleque et al. (2015).

In this methodology, the boundary  $\partial\Omega$  is discretised into  $N_e$  elements of surface  $\partial\Omega_e$ , so the PE boundary integral equation can be written as

$$c_{JK}(\mathbf{x}')u_J(\mathbf{x}') + \sum_{e=1}^{N_e} \left\{ \int_{\partial\Omega_e} T_{JK}(\mathbf{x}', \mathbf{x})u_J(\mathbf{x})dS \right\} = \sum_{e=1}^{N_e} \left\{ \int_{\partial\Omega_e} U_{JK}(\mathbf{x}', \mathbf{x})t_J(\mathbf{x})dS \right\}. \quad (10)$$

In equation (10), upper-case sub-indices range from 1 to 4, so that an extended displacement vector  $u_J$  is defined as

$$u_J = \begin{cases} u_j & J \leq 3 \\ \varphi & J = 4, \end{cases} \quad (11)$$

and an the extended traction vector as

$$t_J = \begin{cases} t_j & J \leq 3 \\ q & J = 4. \end{cases} \quad (12)$$

Matrix  $c_{JK}$  depends on the local geometry of the boundary  $\partial\Omega$  at the collocation point  $\mathbf{x}'$  and is equal to  $\frac{1}{2}\delta_{JK}$  for smooth boundaries (see Mantič, 1993 for non-smooth cases),  $\delta_{JK}$  being the Kronecker delta; and,  $U_{JK}$  and  $T_{JK}$  are the extended displacement fundamental solution and the extended traction fundamental solution, respectively. That is,  $U_{JK}$  represents the elastic displacement, in an infinite PE solid, at the point  $\mathbf{x}$  in the  $x_J$ -direction ( $J = 1 - 3$ ) due to a mechanical force applied at the point  $\mathbf{x}'$  in  $x_K$ -direction ( $K = 1 - 3$ ) or due to a point electric charge ( $K = 4$ ) applied at the point  $\mathbf{x}'$ ; and the electric potential at point  $\mathbf{x}$  ( $J = 4$ ) due to a mechanical force applied at the point  $\mathbf{x}'$  in  $x_K$ -direction ( $K = 1 - 3$ ) or due to a point electric charge ( $K = 4$ ) applied at the point  $\mathbf{x}'$ . Analogously,  $T_{JK}$  is, in an infinite PE solid, the mechanical traction on a plane with outward unit normal to the boundary at the point  $\mathbf{x}$  in the  $x_J$ -direction ( $J = 1 - 3$ ) due to a mechanical force applied at the point  $\mathbf{x}'$  in  $x_K$ -direction ( $K = 1 - 3$ ) or due to a point electric charge ( $K = 4$ ) applied at the point  $\mathbf{x}'$ ; and the electric charge flux on a plane with outward unit normal to the boundary at the point  $\mathbf{x}$  ( $J = 4$ ) due to a mechanical force applied at the point  $\mathbf{x}'$  in  $x_K$ -direction ( $K = 1 - 3$ ) or due to a point electric charge ( $K = 4$ ) applied at the point  $\mathbf{x}'$ . In this work, the scheme for the evaluation of the extended fundamental solutions proposed by Buroni and Sáez (2010) is implemented, which posses the remarkable characteristics that it is exact, explicit and valid for mathematical degenerate and non-degenerate materials in the Stroh formalism context. The strongly singular integral on the left-hand side is evaluated in the Cauchy principal value sense, whereas the

weakly singular integral on the right-hand side is evaluated as an improper integral.

The physical variables  $u_j$  and  $t_j$  are approximated over each element  $\partial\Omega_e$  using linear shape functions, as a function of the nodal values as

$$u_j = \sum_{i=1}^4 N_i(\xi, \eta) u_j^i, \quad (13)$$

$$t_j = \sum_{i=1}^4 N_i(\xi, \eta) t_j^i, \quad (14)$$

where  $u_j^i$  and  $t_j^i$  are the nodal extended displacements and tractions, respectively. After a collocation procedure at boundary nodes and using the approximation (13) and (14), Equation (10) can be written in matricial form as

$$\mathbf{H}\mathbf{u} = \mathbf{G}\mathbf{t}, \quad (15)$$

where vectors  $\mathbf{u}$  and  $\mathbf{t}$  contain the values of all nodal extended displacements and tractions, respectively (i.e.  $\mathbf{u}$  contains the nodal displacements and electric potentials, and  $\mathbf{t}$  contains the nodal tractions and electric charges). Boundary conditions can be imposed rearranging the columns in  $\mathbf{H}$  and  $\mathbf{G}$ , and passing all the unknowns to vector  $\mathbf{x}$  on the left-hand side, resulting in the final system

$$\mathbf{A}\mathbf{x} = \mathbf{F}. \quad (16)$$

### Discrete PE contact formulation

The boundary element approximation for PE contact problems (16) can be rearranged as:

$$\left[ \mathbf{A}_{x_e} \quad \mathbf{A}_{u_c} \quad \mathbf{A}_{\varphi_c} \quad \mathbf{A}_{p_c} \quad \mathbf{A}_{q_c} \right] \left\{ \begin{array}{l} \mathbf{x}_e \\ \mathbf{u}_c \\ \varphi_c \\ \mathbf{p}_c \\ \mathbf{q}_c \end{array} \right\} = \mathbf{F}, \quad (17)$$

where  $\mathbf{x}_e$  collects the nodal external unknowns (i.e., the nodal unknowns which are outside the contact zone),  $\mathbf{u}_c$  and  $\varphi_c$  collect the nodal contact displacements and electric potentials, respectively,  $\mathbf{p}_c$  contains the normal nodal contact tractions (i.e.  $\mathbf{p}_c = \mathbf{p}_v$ ) and  $\mathbf{q}_c$  contains the nodal electric charges. Matrices  $\mathbf{A}_{x_e}$ ,  $\mathbf{A}_{u_c}$ ,  $\mathbf{A}_{\varphi_c}$ ,  $\mathbf{A}_{p_c}$  and  $\mathbf{A}_{q_c}$  are constructed with the columns of matrices  $\mathbf{H}$  and  $\mathbf{G}$ .

Next, nodal electric charge on every contact node  $i$  can be expressed in terms of the electric potential according to the electrical contact condition (6) and (9), as:

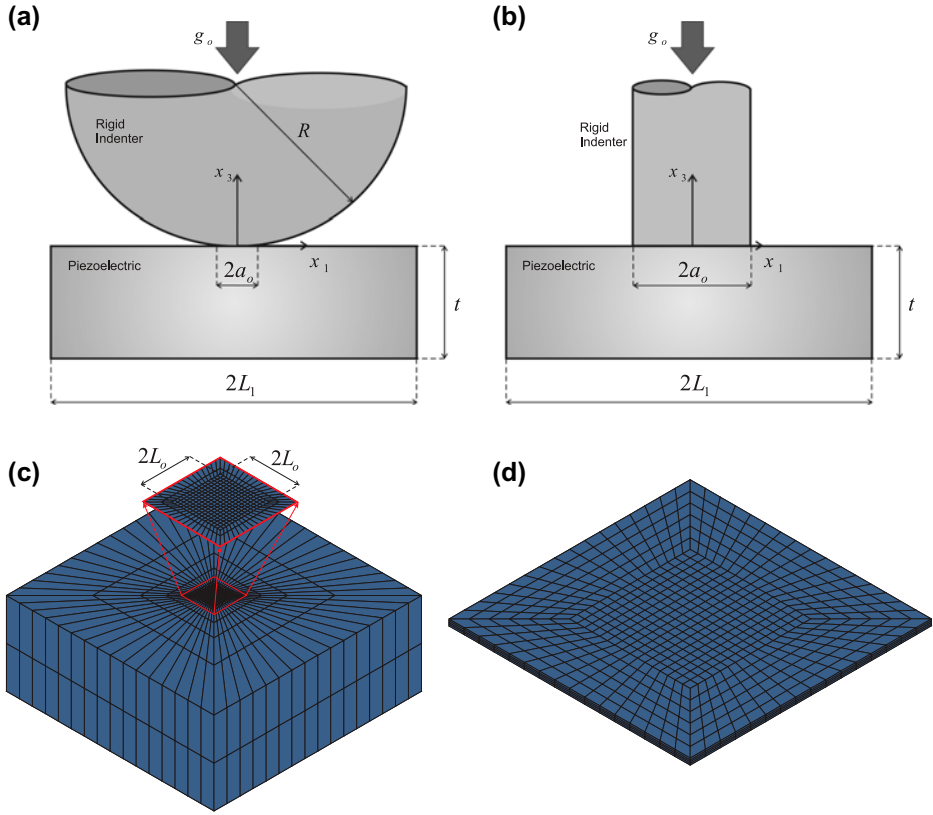


**Figure 1.** (a) Spherical indenter. (b) Flat circular indenter. Boundary element mesh for a half-space configuration (c) and a thin film configuration (d).

$$(\mathbf{q}_c)_i = -\kappa((\mathbf{p}_c)_i)((\varphi_c)_i - (\varphi_o)_i). \quad (18)$$

So equation (17) can be written as

$$\begin{bmatrix} \mathbf{A}_{x_e} & \mathbf{A}_{u_c} & \tilde{\mathbf{A}}_{\varphi_c} & \mathbf{A}_{p_c} \end{bmatrix} \begin{Bmatrix} \mathbf{x}_e \\ \mathbf{u}_c \\ \varphi_c \\ \mathbf{p}_c \end{Bmatrix} = \tilde{\mathbf{F}}, \quad (19)$$

where  $\tilde{\mathbf{A}}_{\varphi_c} = \mathbf{A}_{\varphi_c} - \kappa(\mathbf{p}_c)\mathbf{A}_{q_c}$ ,  $\tilde{\mathbf{F}} = \mathbf{F} - \kappa(\mathbf{p}_c)\mathbf{A}_{q_c}\varphi_o$  and  $\kappa(\mathbf{p}_c)$  is a diagonal matrix, i.e.:  $\kappa(\mathbf{p}_c) = \text{DIAG}(\kappa((\mathbf{p}_c)_1), \dots, \kappa((\mathbf{p}_c)_i), \dots, \kappa((\mathbf{p}_c)_{N_c}))$ .

Finally, the mechanical contact restriction (8) is defined on every contact node  $i$  as:

$$(\mathbf{p}_c)_i - \mathbb{P}_{\mathbb{R}_-}((\mathbf{p}_c)_i + r_v(\mathbf{g}_c)_i) = 0, \quad (20)$$

where  $\mathbf{p}_c$  contains the normal contact tractions of every contact node  $i$  and  $\mathbf{g}_c$  contains the normal gap vector of every contact node  $i$ :  $(\mathbf{g}_c)_i = (\mathbf{g}_o)_i - (\mathbf{u}_c)_i$ .

**Table 1.** Material properties of the PE ceramic BaTiO<sub>3</sub>.

Elastic coefficients (GPa)	
$c_{1111}$	150.00
$c_{1122}$	66.00
$c_{1133}$	66.00
$c_{3333}$	146.00
$c_{2323}$	44.00
Piezoelectric coefficients (C/m <sup>2</sup> )	
$e_{113}$	11.40
$e_{333}$	17.50
$e_{311}$	-4.350
Dielectric constants (10 <sup>-9</sup> F/m)	
$\epsilon_{11}$	9.868
$\epsilon_{33}$	11.151

The quasi-static PE contact problem is thus defined by Equations (19)–(20) and it can be solved using different solution schemes according to Alart and Curnier (1991) and Christensen et al. (1998). In this work, the nonlinear system (19-20) is solved using a well-known iterative method, namely Uzawa's method. This iterative scheme was presented by Kikuchi and Oden (1988) and Alart and Curnier (1991) and later applied to contact of PE materials by Rodríguez-Tembleque et al. (2015).

## Numerical examples

This section studies the indentation response of a transversely isotropic PE block, whose dimensions are  $2L_1 \times 2L_1 \times t$ , under different contact conditions (see Figure 1 (a) and (b) where vertical axis  $x_3$  coincides with  $\mathbf{v}_c$ ). In the numerical examples, two rigid indenters (i.e. a sphere of radius  $R = 100 \times 10^{-3}$  m and a flat circular punch of radius  $a_o = 3.2 \times 10^{-3}$  m) are subjected to a normal indentation  $g_o$ . The normal indentation for the spherical indenter is  $g_o = 5 \times 10^{-5}$  m and for the punch is  $g_o = 5 \times 10^{-6}$  m. The PE block is assumed to be ideally bonded at the base ( $x_3 = -t$ ). A transversely isotropic PE material (BaTiO<sub>3</sub>) with the symmetry axis coinciding with  $x_3$ -direction is considered in this case, its properties being presented in Table 1. The domain is discretised by 1024 linear quadrilateral boundary elements, using  $16 \times 16$  elements on the  $L_o \times L_o$  potential contact zone ( $L_o = 5 \times 10^{-3}$  m), as Figure 1(c) shows. In the case of PE film configurations, a more local and refined mesh on the thickness is considered (see Figure 1(d)).

## Insulating indenters

First, we consider insulating electrical boundary conditions for the indenters. Normalised contact pressure distribution as a function of the ratio of the contact radius  $a$  and the thickness of the film ( $a/t$ ) are presented in Figure 2 for a spherical indenter (Figure 2(a)) and a flat cylindrical punch (Figure 2(b)). Images in Figure 2 present an excellent convergence to the limiting cases (i.e. infinitely

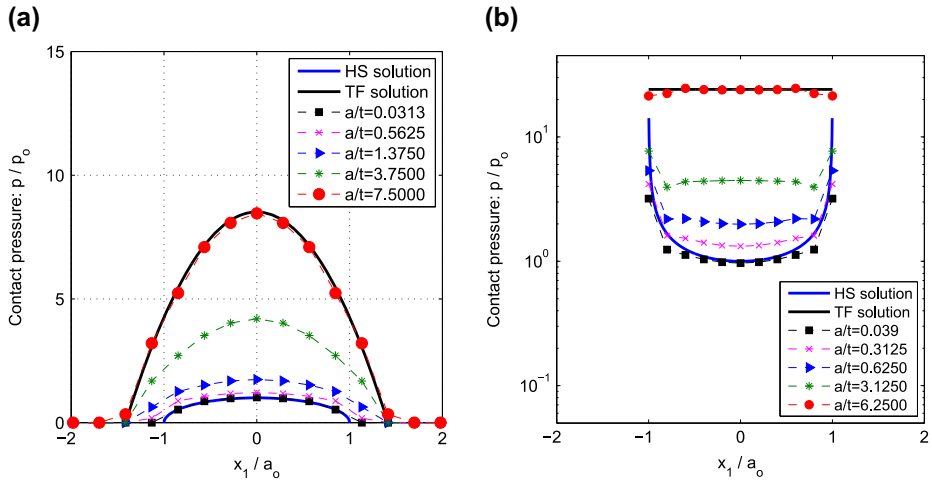


**Figure 2.** Normalised contact pressure distribution as a function of the ratio of the contact radius  $a$  and the thickness of the film ( $a/t$ ) for: (a) spherical indenter and (b) flat circular indenter.

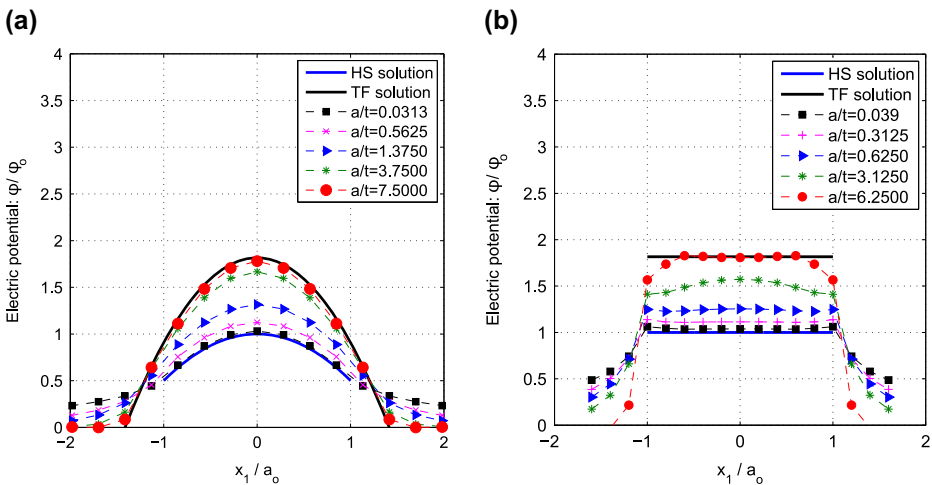


**Figure 3.** Normalised electric potential distribution as a function of the ratio of the contact radius  $a$  and the thickness of the film ( $a/t$ ) for: (a) spherical indenter and (b) flat circular indenter.

thick or half-space (HS) solution and infinitely thin films (TF) solution) when the thickness of the film is augmented or reduced, respectively. Same effects are observed in Figure 3 for the electric potential distribution on each case.

Indentation responses of a finitely thick PE film (i.e. indentation force responses and electric potential) are shown in Figure 4 for the spherical indenter. It may be seen that the transition occurs at around  $a/t \simeq 1$ . HS solutions are good approximation of the indentation responses of a finitely thick PE film when  $a/t < 0.1$ , whilst solutions for an infinitely thin film are more appropriate when  $a/t \simeq 10$ . These conclusions were presented in Wang et al. (2008) for an

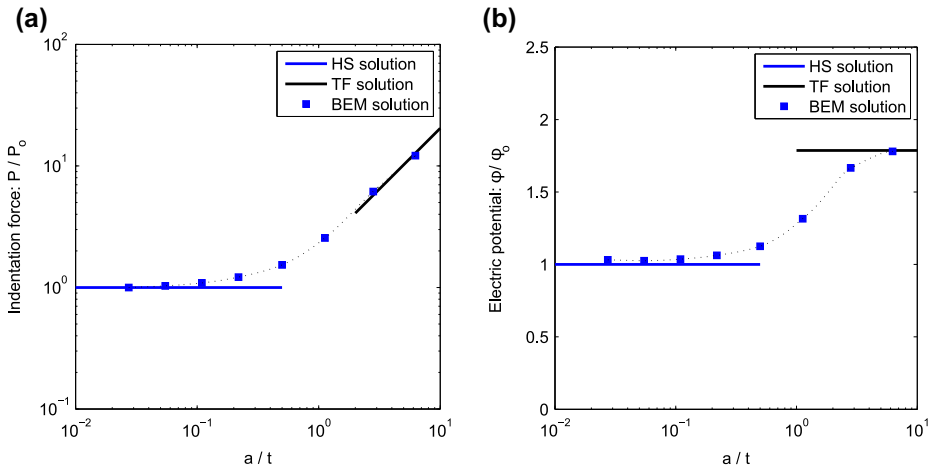


**Figure 4.** Spherical indentation response as a function of the ratio of the contact radius  $a$  and the thickness of the film ( $a/t$ ): (a) Normalised indentation force and (b) Normalised maximum electric potential.

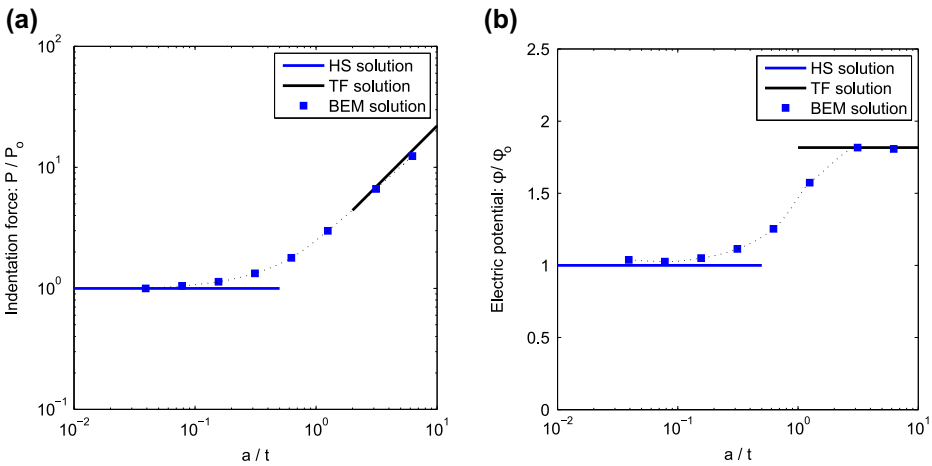


**Figure 5.** Circular cylindrical punch indentation response as a function of the ratio of the contact radius  $a$  and the thickness of the film ( $a/t$ ): (a) Normalised indentation force and (b) Normalised maximum electric potential.

axisymmetric frictionless insulating indentation of finitely thick PE films. Same results are observed in Figure 5 for the punch.

### Conducting indenters

Finally, the influence of the non-isolated indentation conditions are studied for both indenters. The influence of the conductivity parameter  $\kappa^*$  (9) in the indentation force and electric potential are presented in Figures 6 and 7, for a sphere and a punch, respectively. In both cases, a prescribed indenter electric

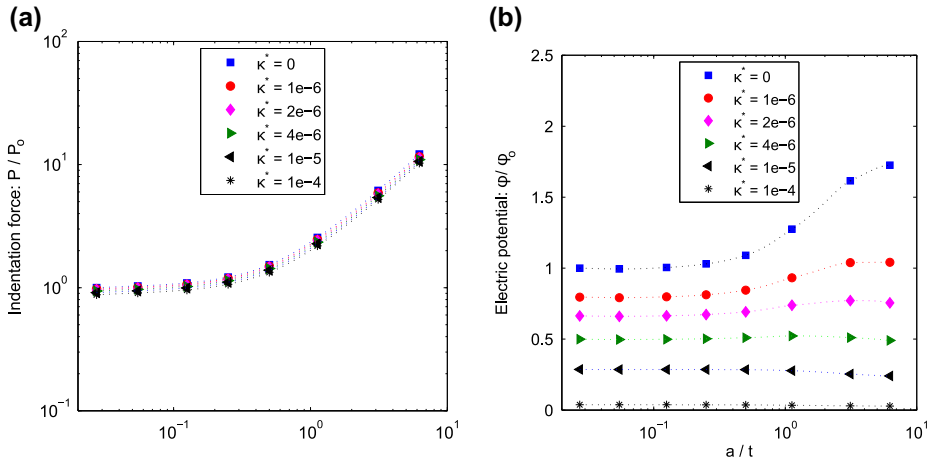


**Figure 6.** Spherical indentation response as a function of the ratio of the contact radius  $a$  and the thickness of the film ( $a/t$ ): (a) Normalised indentation force and (b) Normalised maximum electric potential.

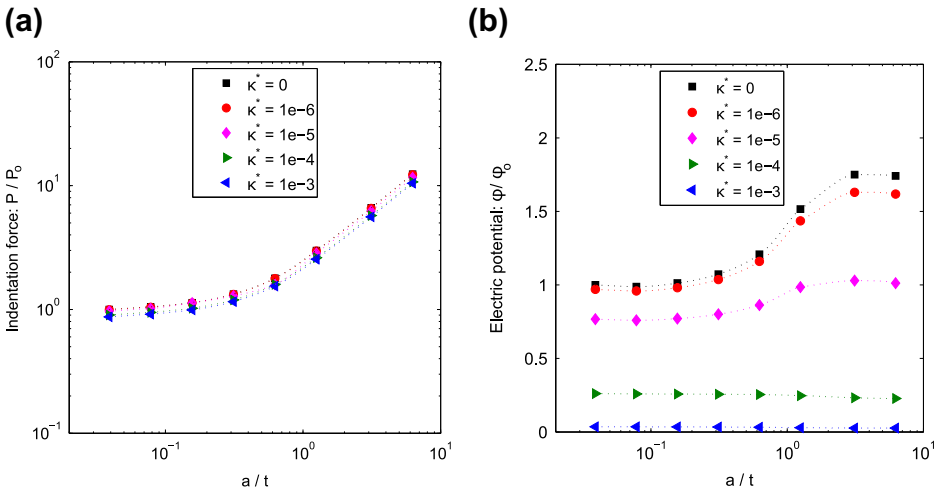


**Figure 7.** Circular cylindrical punch indentation response as a function of the ratio of the contact radius  $a$  and the thickness of the film ( $a/t$ ): (a) Normalised indentation force and (b) Normalised maximum electric potential.

potential is  $\phi_0 = 0$  and the results are normalised relative to the insulating HS indentation.

We observe in Figures 6(a) and 7(a) that indentation forces are not highly affected by the conductivity  $\kappa^*$  in both PE HS and TF configurations. Nevertheless, the values of the electric potential at the contact region are very affected (see Figures 6(b) and 7(b)). They tend to the indenter prescribed electric potential  $\phi_0$  when the values of  $\kappa^*$  are higher, in finitely thick PE films configurations. In fact, when  $\kappa^*$  increases, the influence of  $a/t$  is neglected and PE HS and TF

configurations present the same values for the electric potential at the contact zone.

## Summary

A three-dimensional boundary element formulation has been applied to analyse a transversely isotropic PE material subjected to a normal frictionless indentation. Two kinds of indenters have been considered (i.e. a spherical indenter and a flat cylindrical punch). In both cases, insulating and conducting boundary conditions are studied. Results present an excellent agreement with Wang et al. (2008) for the two limiting cases: infinitely thick and infinitely thin PE films closed-form solutions. Results reveal that the values of the electric potential at the contact region are very affected by ratio  $a/t$  under insulating indentation conditions. For a conducting indenter, electric potential tends to the indenter prescribed electric potential when the values of the conductivity ( $\kappa^*$ ) are higher, but, when  $\kappa^*$  increases, the influence of  $a/t$  is neglected and PE HS and TF configurations present the same values for the electric potential.

## Disclosure statement

No potential conflict of interest was reported by the authors.

## Funding

This work is supported by the *Ministerio de Ciencia e Innovación* (Spain) through the research project [DPI2013-43267-P]; Plan Propio de la Univ. de Sevilla [PP2015-4585].

## ORCID

Luis Rodríguez-Tembleque  <http://orcid.org/0000-0003-2993-8361>

Federico C. Buroni  <http://orcid.org/0000-0001-9746-9478>

Andrés Sáez  <http://orcid.org/0000-0001-5734-6238>

## References

- Alart, P., & Curnier, A. (1991). A mixed formulation for frictional contact problems prone to Newton like solution methods. *Computer Methods in Applied Mechanics and Engineering*, 92, 353–375.
- Aliabadi, M. H. (2002). The boundary element method, *Applications in solids and structures* (Vol. 2). Chichester: John Wiley & Sons.
- Barboteu, M., Fernández, J., & Ouafik, Y. (2008). Numerical analysis of two frictionless elastic-piezoelectric contact problems. *Journal of Mathematical Analysis and Applications*, 339, 905–917.
- Blazquez, A., Mantic, V., & París, F. (2006). Application of BEM to generalized plane problems for anisotropic elastic materials in presence of contact. *Engineering Analysis with Boundary Elements*, 30, 489–502.
- Brebbia, C. A., & Dominguez, J. (1992). *Boundary elements: An introductory course* (2nd ed.). Southampton: WIT Press.

- Buroni, F., & Sáez, A. (2010). Three-dimensional Green's function and its derivative for materials with general anisotropic magneto-electro-elastic coupling. *Proceedings of the Royal Society A*, 466, 515–537.
- Cady, W. (1946). *Piezoelectricity*. New York: McGraw-Hill.
- Chen, W., & Ding, H. (1996). Indentation of a transversely isotropic piezoelectric half-space by a rigid sphere. *Acta Mechanica Solida Sinica*, 12, 114–120.
- Chen, W., Shioya, T., & Ding, H. (1999). The elastoelectric field for a rigid conical punch on a transversely isotropic piezoelectric half-space. *ASME Journal of Applied Mechanics*, 66, 764–771.
- Christensen, P., Klarbring, A., Pang, J. S., & Strömberg, N. (1998). Formulation and comparison of algorithms for frictional contact problems. *International Journal for Numerical Methods in Engineering*, 42, 145–173.
- Ding, H., & Chen, W. (2001). *Three dimensional problems of piezoelectricity*. New York: Nova Science Publishers.
- Ding, H., Hou, P., & Guo, F. (2000). The elastic and electric fields for three-dimensional contact for transversely isotropic piezoelectric materials. *International Journal of Solids and Structures*, 37, 3201–3229.
- Fan, H., Sze, K., & Yang, W. (1996). Two-dimensional contact on a piezoelectric half-space. *International Journal of Solids and Structures*, 33, 1305–1315.
- Gao, C., & Noda, N. (2004). Green's functions of a half-infinite piezoelectric body: Exact solutions. *Acta Mechanica*, 172, 169–179.
- Giannakopoulos, A., & Suresh, S. (1999). Theory of indentation of piezoelectric materials. *Acta Materialia*, 47, 2153–2164.
- Han, W., Sofonea, M., & Kazmi, K. (2007). Analysis and numerical solution of a frictionless contact problem for electro-elastic-visco-plastic materials. *Computer Methods in Applied Mechanics and Engineering*, 196, 3915–3926.
- Hüeber, S., Matei, A., & Wohlmuth, B. (2013). A contact problem for electro-elastic materials. *Zeitschrift für Angewandte Mathematik und Mechanik*, 93, 789–800.
- Ikeda, T. (1996). *Fundamentals of piezoelectricity*. Oxford: Oxford Science Publications.
- Kalinin, S., Karapetian, E., & Kachanov, M. (2004). Nanoelectromechanics of piezoresponse force microscopy. *Physical Review B*, 70, 184101-1–184101-24.
- Kamble, S., Kubair, D., & Ramamurty, U. (2009). Indentation strength of a piezoelectric ceramic: Experiments and simulations. *Journal of Materials Research*, 24, 925–934.
- Ke, L. L., Yang, J., Kitipornchai, S., & Wang, Y. S. (2008). Electro-mechanical frictionless contact behavior of a functionally graded piezoelectric layered half-space under a rigid punch. *International Journal of Solids and Structures*, 45, 3313–3333.
- Kikuchi, N., & Oden, J. (1988). *Contact problems in elasticity: A study of variational inequalities and finite element methods*. Philadelphia: SIAM.
- Laursen, T. (2002). *Computational contact and impact mechanics*. Berlin Heidelberg: Springer.
- Liu, M., & Fuqian, Y. (2012a). Electromechanical behaviour of a finite piezoelectric layer under a flat punch. *Smart Materials and Structures*, 21, 105020(10pp).
- Liu, M., & Fuqian, Y. (2012b). Finite element analysis of the spherical indentation of transversely isotropic piezoelectric materials. *Modelling and Simulation in Materials Science and Engineering*, 20, 045019(15pp).
- Liu, M., & Yang, F. (2013). Three-dimensional finite element simulation of the Berkovich indentation of a transversely isotropic piezoelectric material: Effect of material orientation. *Modelling and Simulation in Materials Science and Engineering*, 21, 045014 (14pp).
- Mantič, V. (1993). A new formula for the C-matrix in the Somigliana identity. *Journal of Elasticity*, 33, 191–201.

- Mason, W. (1950). *Piezoelectric crystals and their application to ultrasonics*. New York: Van Nostrand-Reinhold.
- Matysiak, S. (1985). Indentation strength of a piezoelectric ceramic: Experiments and simulations. *Bulletin of the Polish Academy of Sciences*, 33, 25–34.
- Muralt, P. (2008). Recent progress in materials issues for piezoelectric MEMS. *The American Ceramic Society*, 91, 1385–1396.
- Pohanka, R., & Smith, P. (1988). *Electronic ceramics, properties, devices and applications*. New York: Marcel Dekker.
- Ramamurty, U., Sridhar, S., Giannakopoulos, A. E., & Suresh, S. (1999). An experimental study of spherical indentation of piezoelectric materials. *Acta Materialia*, 47, 2417–2430.
- Ramirez, G. (2006). Frictionless contact in a layered piezoelectric media characterized by complex eigenvalues. *Smart Materials and Structures*, 15, 1287–1295.
- Ramirez, G., & Heyliger, P. (2003). Frictionless contact in a layered piezoelectric half-space. *Smart Materials and Structures*, 12, 612–625.
- Rodríguez-Tembleque, L., Buroni, F. C., Abascal, R., & Sáez, A. (2011). 3D frictional contact of anisotropic solids using BEM. *European Journal of Mechanics A Solids*, 30, 95–104.
- Rodríguez-Tembleque, L., Buroni, F., & Sáez, A. (2015). 3D BEM for orthotropic frictional contact of piezoelectric bodies. *Computational Mechanics*, 56, 491–502.
- Saigal, A., Giannakopoulos, A. E., Pettermann, H. E., & Suresh, S. (1999). Electrical response during indentation of a 1–3 piezoelectric ceramic-polymer composite. *J. Appl. Phys.*, 86, 603–6.
- Uchino, K. (1997). *Piezoelectric actuators and ultrasonic motors*. Boston MA: Kluwer Academic.
- Wang, J., Chen, C., & Lu, T. (2008). Indentation responses of piezoelectric films. *Journal of the Mechanics and Physics of Solids*, 56, 3331–3351.
- Wang, J., Chen, C., & Lu, T. (2011). Indentation responses of piezoelectric films ideally bonded to an elastic substrate. *International Journal of Solids and Structures*, 48, 2743–2754.
- Wang, J., Fang, S., & Chen, L. (2002). The state vector methods for space axisymmetric problems in multilayered piezoelectric media. *International Journal of Solids and Structures*, 38, 3959–3970.
- Wang, B., & Han, J. (2006). A circular indenter on a piezoelectric layer. *Archive of Applied Mechanics*, 76, 367–379.
- Wang, J., Lu, T., & Chen, C. (2012). Indentation responses of piezoelectric films ideally bonded to an elastic substrate. *International Journal of Solids and Structures*, 49, 95–110.
- Wriggers, P. (2002). *Contact problems in elasticity: A study of variational inequalities and finite element methods*. Chichester: John Wiley & Sons.
- Yang, F. (2008). Analysis of the axisymmetric indentation of a semi-infinite piezoelectric material: the evaluation of the contact stiffness and the effective piezoelectric constant. *Journal of Applied Physics*, 103, 074115.
- Yang, J., & Yang, J. (2005). *An introduction to the theory of piezoelectricity*. New York: Springer.